Osmotic compression and stiffness changes in relaxed skinned cardiac myocytes in PVP-40 and Dextran T-500

Kenneth P. Roos and Allan J. Brady
Department of Physiology and the Cardiovascular Research Laboratory, University of California at Los Angeles, School of Medicine, Los Angeles, California 90024-1760 USA

ABSTRACT Sarcomere lengths, cell widths, indices of stiffness, and striation pattern uniformity were determined from radially compressed isolated adult cardiac myocytes from the rat. Single cells were bathed in a series of relaxing solutions containing 0–15% concentrations of nonpenetrating long chain polymers PVP-40 and dextran T-500. There were no significant changes observed in average sarcomere lengths or in striation pattern uniformity at any concentration. But cell widths decreased and stiffness increased in both polymers in a concentration-osmotic pressure-dependent relationship. Changes in cell width and stiffness were repeatable in either polymer, but only after an initial compression with a 10 or 15% concentration solution. The observed reduction in cell width after initial compression correlates well with known myofilament lattice spacing compression in rat cardiac muscle and is qualitatively similar to compressions seen in skeletal muscle preparations. But the cardiac myofilament lattice may not be as compressible as the skeletal lattice. Like skeletal muscle, stiffness exhibits a two-phase relationship where most of the increase occurs at solution osmotic pressures >20 Torr. Finally, the inherently greater passive stiffness-length relationship of cardiac muscle is maintained at higher osmotic pressures such that the passive elastic modulus is strongly length dependent.

INTRODUCTION

Single skeletal muscle fibers swell by 8–28% when their sarcolemma is disrupted or removed in relaxing solution (7, 8, 15, 18, 20, 21, 28). This observation has been attributed to the loss of the osmotic constraint on cell volume upon skinning (15). Cell diameter and lattice spacing can be modulated and returned to normal levels with the addition of long chain polymers such as PVP-40 or dextran T-500 which appear to be excluded from the myofilament lattice in skinned cells permitting osmotic compression. This approach has been used extensively to modulate lattice spacing in skinned skeletal muscle cells for the controlled investigation of stiffness modulus, force, and structural properties of the contractile apparatus (1, 7–13, 15, 18, 20, 23–25, 28, 34, 35).

As opposed to skeletal muscle, there is very little data on the swelling or recompression of cardiac muscle cells and its effect upon force or stiffness. Matsubara and Millman (17) reported that x-ray diffraction patterns from intact mammalian heart muscle were qualitatively similar to those of frog skeletal muscle. These data were indicative of an hexagonal myofilament lattice whose spacing varied with sarcomere length in an isovolumetric manner. Fabiato and Fabiato (4) indicated that their mechanically skinned cardiac fibers were swollen relative to their intact size. A 10% PVP-40 solution reduced their preparation width by 21% and its maximum force production by ~25%. Maughan and Berman (19) subsequently reported that only a 7% cell width reduction was necessary to reduce active force by 25% in chemically skinned cardiac muscle bundles. Furthermore, they found that cell force was completely abolished when cell width was reduced by one-third. Recently, Matsubara et al. (16) examined x-ray diffraction patterns from saponin-treated rat papillary muscles and reported that the d_{10} lattice spacing increased by 8% (35.6 to 38.4 nm) over intact muscles in the 2.1–2.25 μm sarcomere length range. They also found that contrary to their findings in mammalian skeletal muscle (18), a significant fraction of the myosin heads appear to be shifted toward the thin filaments at low Ca^{2+} concentrations but do not produce tension. Matsubara and Maughan (personal communication, see acknowledgment) have indicated that some of their saponin-treated rat papillary muscles (16) were also osmotically compressed with dextran T-500. They report that the lattice spacing in the 2.18–2.37 μm sarcomere length range was reduced from an average 38.8 nm in control relaxing solution to ~37.8 nm in a 2% dextran-relaxing solution, 34.5 nm in 4%, 32.2 nm in 7%, and 30.9 nm in 10%; these are respectively, 2.6, 11.1, 17, and 20.4% compressions in lattice spacing relative to the skinned cell.

In this report, we characterize the effects of osmotic compression of the myofilament lattice upon cell width, cell length, stiffness modulus, and sarcomere uniformity for the first time in isolated cardiac myocytes. Because a cardiac myocyte is too small in size to yield useful x-ray diffraction analysis for myofilament lattice spacing deter-

mination, we must rely upon cell width measurements as an index of lattice spacing. One objective of the present study is to determine if cell width measurements can serve as a reasonable indicator of myofilament lattice spacing in isolated skinned cardiac cells as they have in skeletal muscle preparations (1, 7–13, 18, 20, 21, 23–25, 34, 35). And, if so, how do the results compare with previously published cardiac and skeletal muscle data? Comparison between the two muscle types is of interest because they have vastly different cellular proportions of myofibrils (3, 22, 26). The final objective of this study is to determine whether the greater passive stiffness of cardiac muscle preparations from a given species (4, 6) might be reflected in the stiffness response to cell size alterations produced by osmotic compression.

We have previously reported (29) that the size and shape of rat cardiac myocytes with intact membrane systems were sensitive to osmotic stress. But these cells lose their organelles when skinned in Triton X-100 detergent (32) and do not significantly change their size and shape as might be expected from the 8% swelling reported in the myofilament lattice of cardiac papillary muscle (16). Though substantially different from observations in skeletal muscle where both the cell width (7, 8, 20, 21) and the myofilament lattice (15, 18) become swollen upon skinning, these findings do not rule out the reliability of cardiac cell width as an index of myofilament lattice spacing when osmotically compressed.

We have measured cell width, striation pattern uniformity, and an index of stiffness in detergent skinned cardiac myocytes in response to 0–15% concentrations of long chain polymers in relaxing solution. We have used both the PVP-40 and dextran T-500 polymers to permit direct comparison with the widest range of similar data from cardiac and skeletal muscle preparations previously reported in the literature. Our data suggest that cell width can be a useful measure of myofilament lattice spacing under carefully controlled conditions. We find that isolated cardiac myocytes behave similarly to other striated muscle preparations, and the strong length dependence of passive tension characteristic of cardiac muscle is retained in the compressed states.

METHODS

Myocyte preparation

Isolated cardiac myocytes were prepared by coronary artery perfusion (Langendorff) of excised adult rat heart with a 0.1% (wt/vol) collagenase digesting solution. After collagenase treatment, the heart was removed from the perfusion apparatus and placed in a petri dish containing a 0.25-mM Ca^{2+}-Tyrode's saline solution. Adult myocytes were isolated by mincing, agitating, and filtering the digested tissue in perfusate. All cell preparation and maintenance solutions were oxygenated with 98% O_2–2% CO_2 and the pH is adjusted to 7.2 with NaOH and HCl at room temperature (23°C). Complete details of the solution and cell preparation procedures are identical to those recently described elsewhere (32).

For these experiments, the cells were chemically skinned with a 1% (vol/vol) Triton X-100 detergent solution. First, the Tyrode's saline solution was replaced by a K^+-EGTA based relaxing solution modified from Fabiato and Fabiato (5). Our relaxing solution consists of 3.385 ml K_2CaEGTA (10 mM EGTA, 10 mM $CaCO_3$, 30 mM KOH) added to 1 liter of H_2O containing (in millimolar): 35 KOH, 10 EGTA, 30 TES buffer, 58.072 KCl, 8.473 $MgCl_2$, 7 glucose, 12 phosphocreatine, 3.3 ATP, and 15 units/ml creatine phosphokinase (CPK). This solution has a total ionic strength of 0.16 M, and a PCa > 8 to minimize any Ca^{2+} mediated cross-bridge interaction and insure that all cells were fully relaxed (32). Cells were then detergent skinned for 10–20 min to insure disruption of all membrane systems (32). After chemical skinning, the cells were returned to the relaxing solution to await experimental use.

Experimental solutions and protocols

Experiments were initiated by the selection of a single myocyte from a dilute suspension of skinned cells in relaxing solution. After a minute or two, the cells settled onto the bottom of a standard microscope glass slide (for the imaging experiments with unrestrained cells) or a glass bottomed chamber (for the stiffness experiments with attached cells) mounted on the stage of a light microscope (Carl Zeiss Inc., Thornwood, NY). Cells were selected according to previously described criteria (31). Rectangular cell shape was particularly critical in these experiments to insure interpretable width and stiffness data. In some experiments, cells were selected in the Tyrode's solution, tested for excitability, relaxed, and skinned under the microscope objective. There were no differences in average cell size, shape, uniformity, and stiffness characteristics between these two selection methods. Control conditions for all experiments were with skinned relaxed cells.

After selection, each cell was exposed to a series of relaxing solutions containing 0–15% (wt/vol) concentrations (e.g., 0–15 gms/100 ml) of nonpenetrating, long-chain polymers. We used either polyvinylpyrrolidone (PVP-40, Sigma Chemical Co., St. Louis, MO) or dextran (T-500, Pharmacia Fine Chemicals, Piscataway, NJ) to osmotically modulate the skinned cell width. Two experimental protocols were applied to the ordering of solution exchanges: independent and stepwise. In the independently ordered experiments, each exposure to a polymer solution was separated by an exposure to the control (0% polymer in) relaxing solution (e.g., 0, 10, 0, 3, 0, 8, and so on). In the stepwise ordered experiments, the cell was first exposed to increasingly large concentrations of polymer solution without interruption by the control solution (e.g., 0, 2, 3, 4, 6, 8, 10, and 15%); this was followed by a stepwise reduction in polymer concentrations back to control relaxing solution.

Because of the syrup-like consistency of the higher concentration polymer solutions, it was critical to insure complete exchange. Therefore we used a multi-port injection/vacuum suction system integrated into the stiffness measurement chamber, or manual injection/vacuum suction around the objective on the glass slide (32). In either case, the solutions were introduced in multiple places while the excess media is pulled off. Reproducible data usually required at least two solution exchanges over a period of several minutes to insure complete replacement of bathing media. Furthermore, cell image data were obtained at least twice in each solution to insure completion of any size or shape changes; stiffness data were monitored continuously. It was found that most cells required at least 10–15 min after a second solution exchange before stabilizing. Therefore most image data were acquired with at least 20 min total exposure to each solution.

Data acquisition and analysis

To measure sarcomere striation spacing, cell widths, and striation pattern uniformity, Nomarski DIC enhanced images of unrestrained myocytes were photographed with a 35-mm camera (OM-2N; Olympus, Woodbury, NY) and digitally imaged with a striation pattern detection system (29–33) in each solution. High contrast photographic enlargements were made from black and white negative film (Kodabromide F4 paper and TP-2415 film; Eastman Kodak, Rochester, NY) for length and width analysis (29) as in Figs. 1–3. These micrographs were measured in at least three locations to determine changes in average striation spacing and cell width. Single line striation pattern intensity profiles from digital recordings were processed to obtain additional striation spacing measurements from each cell (33). There were no significant differences between average striation spacing data derived from photomicrographic measurement or digital images. All measurements were calibrated to a 2.0-μm stage micrometer (Graticules Ltd., Tonbridge, UK). Average striation spacing data were determined to better than 0.5% whereas individual cell widths were measured to better than 2%. Solution osmotic pressures at each PVP and dextran concentration were estimated for Fig. 3 *B* from the equations of Vink (36) and Fig. 1 of Millman et al. (24).

For the striation pattern uniformity determination, a planar map was reconstructed from a raster series of single line intensity profile images (30, 33). These data are then processed and two-dimensionally reconstructed with color coded striation spacing to assist in visualization of uniformity as in Fig. 4. These two-dimensional data were also statistically analyzed for regional sarcomere length distribution (31).

An index of cell stiffness was determined from myocytes attached to a piezoelectric length perturbator and a tension transducer with double-barreled suction micropipettes (See Fig. 1, reference 2). Sinusoidal length perturbations (1–1.5% at 70 Hz) were applied at one end and the tension measured at the other end. Overall cell length was controlled by micromanipulators upon which the perturbator and transducer sit. Stiffness is calculated on-line with a lock-in amplifier as the ratio of the induced force changes to the length perturbation amplitude. Tension and stiffness changes were simultaneously recorded with a chart recorder (Graphtec, WR-3101, Irvine, CA) and logged into a digital computer (Rainbow 100, Digital Equipment Corp., Maynard, MA) for later analysis (2, 32). Cell stiffness was normalized from the pooled data recorded in control relaxing solution (0% polymer) at slack length (L_0) as presented in Figs. 5–7.

RESULTS

Average sarcomere lengths, cell widths, and striation pattern uniformity were obtained from 57 unrestrained myocytes and an index of stiffness from 16 attached myocytes radially compressed with either PVP-40 or dextran T-500.

Cell width changes

Fig. 1 illustrates the changes in cell width with PVP concentration in the same segment of an unrestrained cell. The first panel on the left is the freshly skinned cell in relaxing solution. This is followed by an initial compression with a 15% solution and a return to 0% control solution. The next four panels show the cell in increasing concentrations of PVP and a final 0% control. Cell width is clearly reduced in a concentration-dependent manner while sarcomere length and striation pattern uniformity appear unchanged (also see Fig. 4).

Fig. 1 also demonstrates that this cell's width returns to only ~95% (panel 3) of its original width (panel 1) after

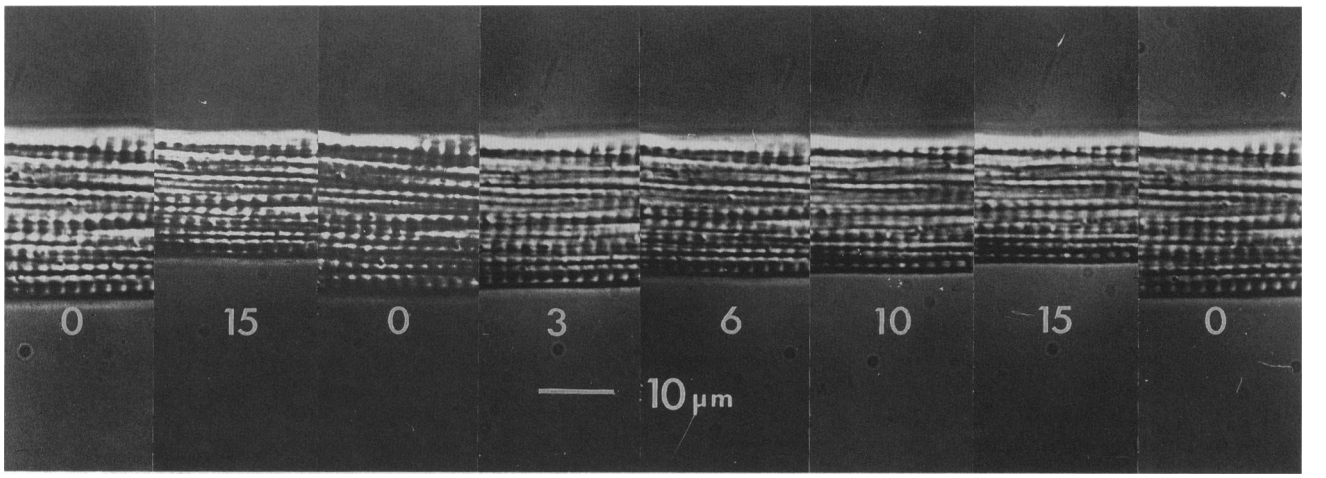

FIGURE 1 Photomicrographs of a relaxed cell in an independently ordered series of PVP-40 solutions. From left to right, segments of cell A-321 are shown in relaxing solutions containing 0, 15, 0, 3, 6, 10, 15, and 0% PVP-40. Each micrograph is the same 21-μm long segment printed at the same magnification. The cell was exposed to each solution for at least 20 min. In this independently ordered experiment, each exposure to a PVP-containing solution was separated by a control exposure to relaxing solution (0%). With the exception of the third and last panels, these control exposures are not shown to better illustrate the modulation of cell width in each concentration of PVP. There was no significant difference between any 0% control solution after the first compression.

an initial compression with 15% PVP. After subsequent compressions, this cell's width returns to an average 0.945 ± 0.04 X of the initial value in the 0% control solution. This behavior was found in all cells examined. Several other cells were even exposed to the control (0%) relaxing solution for over 2 h with solution exchanges every 2 min for the first 20 min and every 10 min thereafter. There was no further re-expansion of cell width after the initial 10 min. For all cells, the average reduction in control cell width after an exposure to 10 or 15% polymer is 0.937 ± 0.012 for PVP-40 and 0.944 ± 0.014 for dextran T-500. All subsequent cell width data (Figs. 2, 3, and 6) has been normalized to these post-initial compression values to adjust for this 6% difference.

Fig. 2 illustrates the average cell width changes as a function of PVP-40 (Fig. 2 *A*) and dextran T-500 (Fig. 2 *B*) concentrations. The average values of the initial compression are designated by open symbols and the dotted lines while subsequent values are drawn with closed symbols and solid lines. The initial compression data are significantly different (at $P < 0.05$) from subsequent compressions in the 0–4% concentration range of either polymer and in 6% PVP ($P = 0.05$).

Fig. 3 replots both the PVP-40 and dextran T-500 cell width data as a function of polymer concentration (Fig. 3 *A*) or log osmotic pressure (Fig. 3 *B*). The lattice compression data of Matsubara and Maughan (personal communication, see acknowledgments) are also shown for comparison normalized on the same axes. There is no significant difference ($P < 0.05$) between the two curves of width data nor from the lattice data (except at 2%) as a function of concentration. But cell widths are significantly different ($P < 0.05$) between all adjacent steps in polymer concentration except the dextran 3.5–5% step ($P = 0.18$). These data show that relaxed cardiac cell width decreases with a curvilinear relationship in response to increasing polymer concentrations. On the other hand, the cell widths are nearly linear with a slope of ~0.10 (relative width units/log decade) when plotted as a function of log osmotic pressure (Fig. 3 *B*). This compares with a somewhat steeper slope of −0.125 in frog sartorius for the dependence of lattice spacing on dextran-induced osmotic pressure (25).

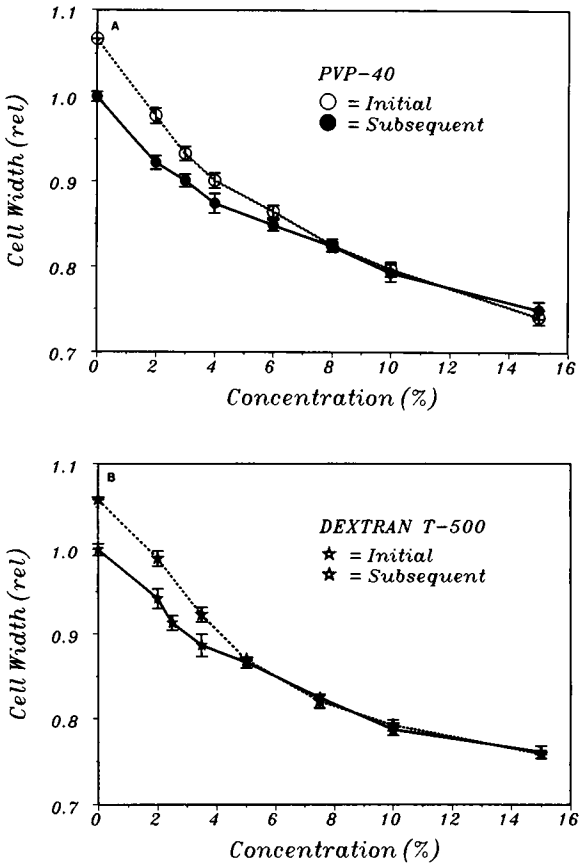

FIGURE 2 Average changes in cell width with PVP-40 and dextran T-500. Average cell width is plotted as a function of PVP-40 (*A*) and dextran T-500 (*B*) concentrations after minimum 20 min. exposures to each concentration. PVP-40 data are illustrated with open and closed circles whereas dextran T-500 data are illustrated with open and closed stars. The open symbols and dashed lines indicate average cell widths from initial compressions in stepwise ordered experiments. The filled symbols and solid lines indicate average cell width data obtained from both stepwise and independent ordered experiments after initial 10 or 15% compressions. Both PVP and dextran data are normalized to their average value in 0% control solution after the initial compression. The error bars indicate standard deviation.

Length and striation pattern uniformity changes

There was no significant change in average sarcomere length when the heart cell was exposed to most concentrations of PVP or dextran. From all the unrestrained cells measured, sarcomere length averaged 1.872 ± 0.038 μm in relaxing solution and 1.877 ± 0.036 μm in 10% concentrations of either polymer. But a small amount of sagging was noted in perturbated attached cells in 12.5 and 15% dextran solutions upon releases back to L_0 from longer lengths.

Furthermore, Fig. 4 shows that there was no major difference in the global pattern of sarcomere length distribution within unrestrained cells at their inherent resting length (L_0) when radially compressed. As previously reported (31), domains of sarcomeres representing the field structure of myofibrils in cardiac muscle (3, 22) can range in size from a few microns to tens of microns in each direction. In Fig. 4, domains of relatively shorter or longer sarcomere lengths are seen in the same areas of the cell image in control, 5%, and 10% dextran solutions despite the changes in cell width. These domains are seen

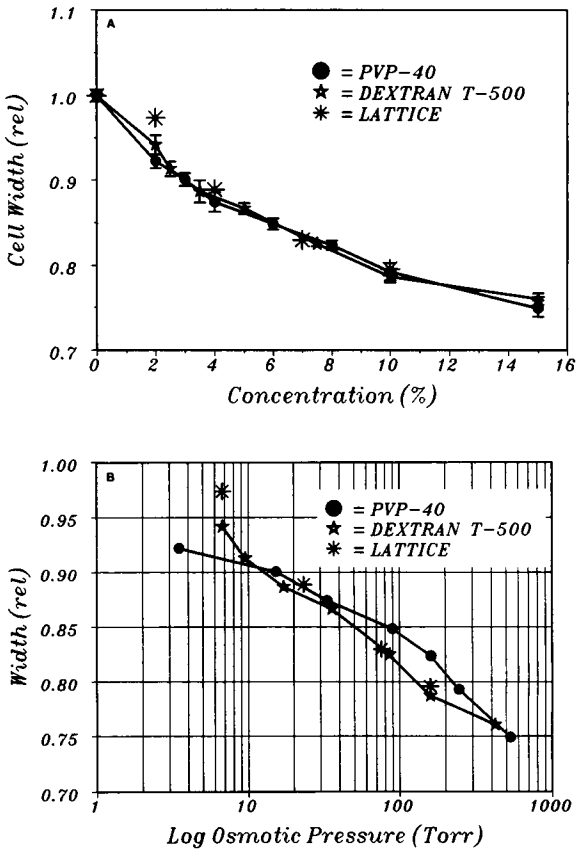

FIGURE 3 Comparison of cell width and myofilament lattice compressions. Final relative cell widths from Figs. 2 are replotted together as a function of (*A*) polymer concentration and (*B*) calculated log osmotic pressure. PVP is represented by solid lines and filled circles while dextran is represented by dash lines and stars. Additionally, the lattice compression data of Matsubara and Maughan (personal communication) are indicated by the asterisk. Both PVP and dextran data are normalized to their average value in 0% control solution after the initial compression. The error bars indicate standard deviation.

as predominantly green/blue/purple vs. red/orange/yellow regions in this figure. For example, the upper left corners defined by width dimensions 11–30 μm and length dimensions 5–35 μm appear more green/blue/purple then red/orange/yellow in these figures. The opposite is true for the lower right corner defined by width dimensions 0–11 μm and length dimensions 40–85 μm. These two domains exhibit significantly different average length periodicities at the $P < 0.001$ level. There are some single point or paired changes in color in these illustrations which reflect the inherent individual striation detection noise of ± 0.05 μm (31).

Stiffness

Relative changes in stiffness modulus are plotted as a function of polymer concentration (Figs. 5), and cell width (Figs. 6), at three different cell lengths: L_0, 105% L_0, and 110% L_0. These responses are not different between PVP or dextran for polymer concentrations < 10%. The baseline (0% PVP at L_0) stiffness level of 6 mN/mm^2 rises nonlinearly with increasing concentration (Fig. 5 *A*); the dextran response is of similar shape and magnitude (Fig. 5 *B*). Also the stiffness is greater in any given concentration at longer initial cell lengths. In general, the stiffness relationship is curvilinear with most of the increase and length dependence effects occurring at concentrations $\geq$5%. This is in contrast to the width response (Fig. 3 *A*) in which the cell diameter has been compressed to 0.86 of control in 5% solutions. The relatively weak dependence of stiffness upon width in low (<5%) concentrations of both polymers is more clearly seen in Fig. 6. Here, most of the stiffness increase occurs at cell widths <0.86. This type of response was also noted in skeletal muscle by Millman and Irving (25) who found that the lattice spacing decreased rapidly with increasing osmotic pressure up to ~20 Torr ($\simeq$ 4% dextran) and then significantly more slowly at higher pressure.

At higher concentrations of dextran, stiffness tends to level off, particularly at L_0. We noted a small amount of sagging (which disappeared after a few minutes) in some attached cells returned to L_0 immediately after small stretches in 15% dextran solutions. This suggests that some elongation may occur in the higher concentrations which would reduce the apparent stiffness measured at fixed cell length. However, we never observed any elongation of unrestrained cells at any concentration or of attached cells in PVP.

DISCUSSION

This study characterizes the effects of osmotic compression for the first time in isolated cardiac myocytes. The primary finding is that nonpenetrating, long-chain polymers PVP-40, and dextran T-500 osmotically change relaxed skinned cardiac cell width and stiffness, but not length or striation pattern uniformity. In general, the effects of osmotic compression on cardiac myocyte width and stiffness are qualitatively similar to those of skeletal muscle. The major differences appeared to be (*a*) in the absolute magnitude of compression at a given osmotic pressure and (*b*) in the strongly length-dependent resting stiffness of the cardiac cells which persisted at the higher osmotic pressures.

Cell width and myofilament lattice compression

Cell width decreases with a curvilinear relationship to increasing concentrations (Fig. 3 *A*) or with a nearly

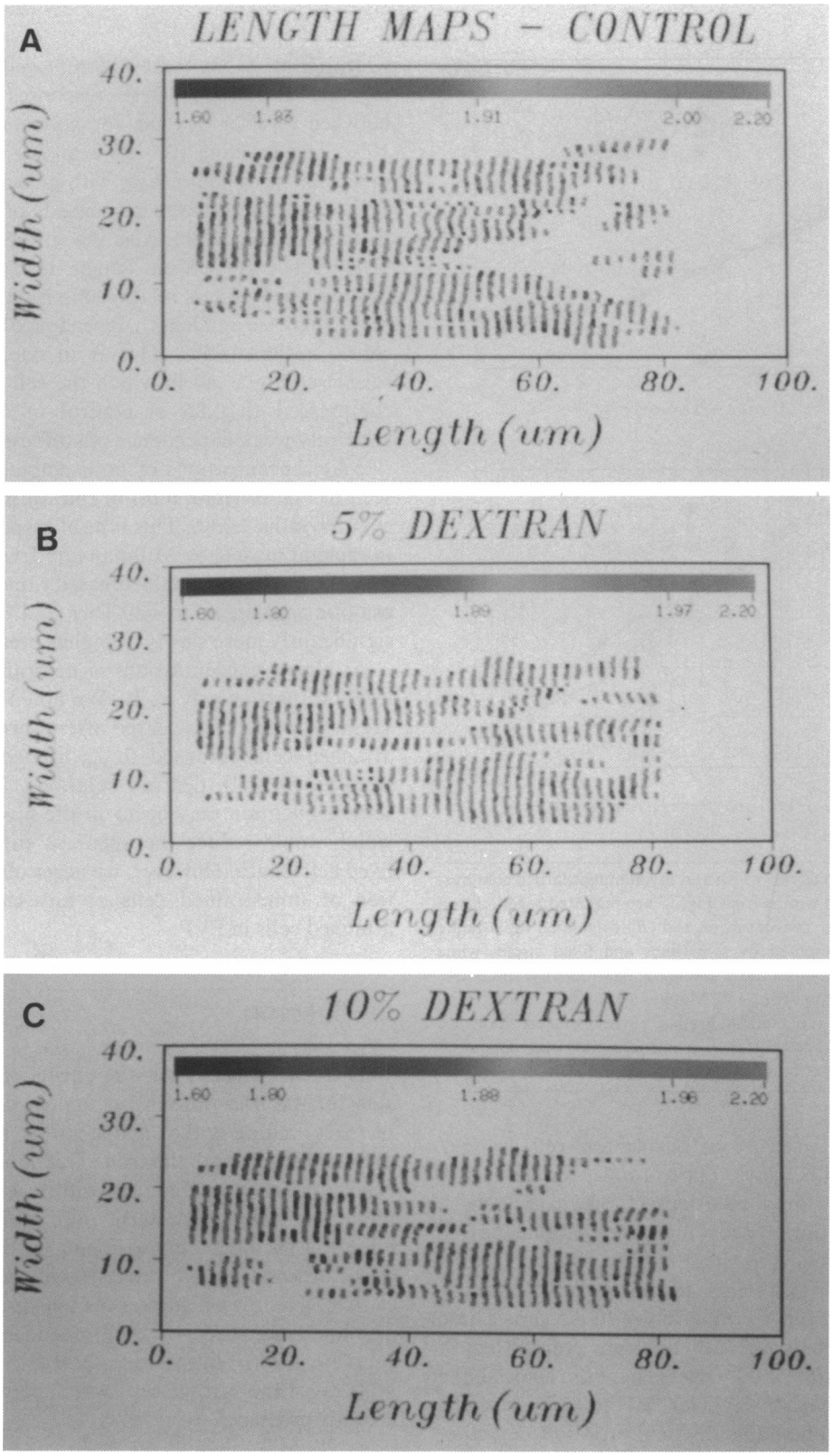

FIGURE 4 Striation pattern uniformity in cells compressed with dextran T-500. Two-dimensional reconstructions of the striation pattern from cell Z-254 are illustrated in (*A*) control relaxing solution (before initial compression), (*B*) in 5% dextran, and (*C*) 10% dextran. These reconstructions depict the central three-fourths of this cell as projected by the microscope onto the image sensor. Clear regions in each plot represent areas with no visible striations. No nuclei are visible at these focal planes. Each striation spacing is assigned a color according to a histogram normalized distribution shown in the table at the top of the illustration. The center number is the mean striation periodicity, the numbers immediately to the right and left designate the standard deviation, and the numbers to the ends indicate the range of color length coding within which all data are contained.

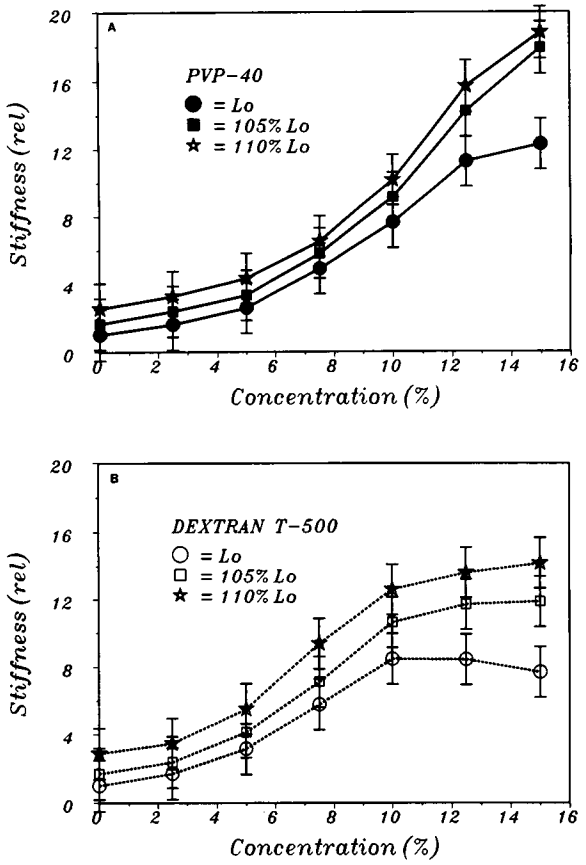

FIGURE 5 Polymer stiffness-concentration relationship. Stiffness changes are plotted at three lengths as a function of (*A*) PVP-40 and (*B*) dextran T-500 concentrations. PVP data are indicated by solid lines while dextran data use dashed lines. The three lengths (L_0, 105% L_0, and 110% L_0) are respectively, designated by circles, squares, and stars. The stiffness data are pooled and normalized to their value in 0% control solution at L_0. Data are from both stepwise and independently ordered experiments.

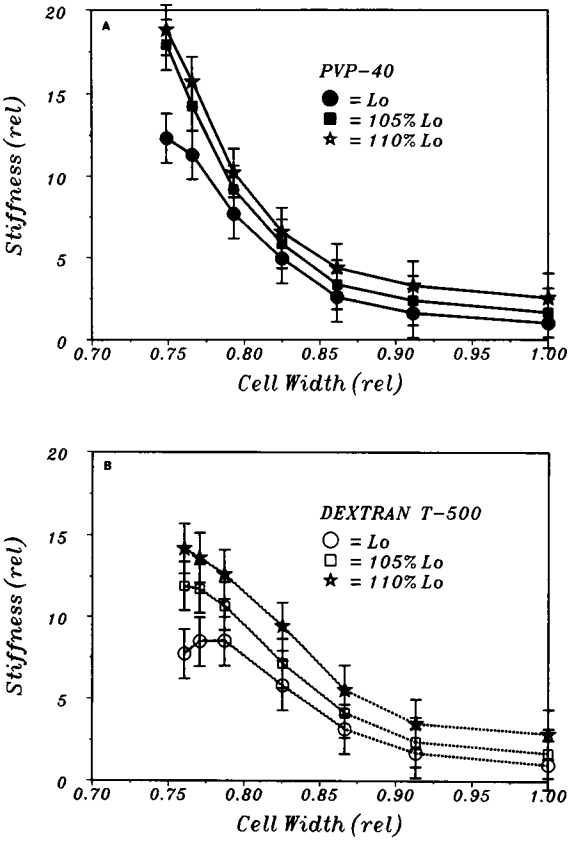

FIGURE 6 Polymer stiffness-width relationship. Stiffness changes are replotted from Fig. 5 at three lengths as a function of normalized cell widths in (*A*) PVP-40 and (*B*) dextran T-500. All symbols and conditions are identical to those in Fig. 5.

linear relationship to increasing log osmotic pressure (Fig. 3 *B*) in either polymer. The magnitude of osmotic radial compression as measured by cell width in any one concentration of polymer is highly dependent on the cell's exposure history. It is clearly necessary to use an adequate solution exchange protocol and to precompress the myocyte with a relatively high concentration (10–15%) of polymer (Fig. 2) to subsequently obtain data that can be reliably correlated to the myofilament lattice spacing (Fig. 3). As shown in Fig. 2, cell widths of freshly skinned cardiac cells appear to be ~6% larger than their final control values and the initial stepwise compressions are significantly different from subsequent compressions (of any kind) in the 0–4% concentration range.

These data suggest that there are residual cellular components (such as mitochondrial debris) remaining in the spaces between the myofibrillar fields of sarcomeres (22) that must be squeezed or wahed out of the cell before its width can be a reliable measure of lattice spacing. It is almost certain that the polymer solutions enter the relatively large interfibrillar spaces, but not significantly into the myofilament lattice within each field (intrafibrillar space). As the polymer solution encounters the cell, water may diffuse from the interfibrillar space more rapidly than from the intrafibrillar space. This could create a transient reduction in interfibrillar space which would tend to exude any residual material from the area. In time, balance would be restored. But the initial transient pumping action may remove residual interfibrillar debris so that the cell size response becomes more reproducible with successive osmotic manipulation. The necessity to initially compress cells is not the exclusive property of cardiac cells. Umazume et al. (35) noted that it was necessary to precompress frog skeletal fibers with

10% PVP K-30 to obtain cell width data that would correlate with their x-ray diffraction lattice spacing data at lower polymer concentrations.

After an initial large osmotic compression, the magnitude of radial compression as measured by cell width (Fig. 3) is in accordance with the myofilament lattice data of Matsubara and Maughan (Introduction) from papillary muscle. For example, at a 10% polymer concentration they noted a 20.4% decrease in lattice spacing while we found a 21% reduction in cell width. Similarly, Fabiato and Fabiato (4) noted a 21% reduction in mechanically skinned cell width in 10% PVP-40. Though these data all have similar proportional reductions in cell width or lattice spacing, the absolute lattice spacings may be different because the data were obtained at different sarcomere lengths.

This close correlation during compression does not apply to the initial 8% swelling of the myofilament lattice upon skinning (16); we found a 1% decrease in cell width from intact to skinned conditions (32). This difference is probably due to loss of most interfibrillar mitochondrial structures after detergent treatment; additional structures may be removed during the initial compression (as previously discussed). Nevertheless, these data indicate that cell width is a reliable index of myofilament lattice spacing in skinned relaxed cardiac cells when measured with the strict protocols described for this study. Additionally, these data suggest (from Fig. 3) that the 8% swelling of the myofilament lattice in a skinned cell can be prevented by about a 2½% (wt/vol) concentration of these polymers.

These findings are qualitatively the same as those found in skeletal muscle. From the equations of Vink (36) and the dashed line in Fig. 1 of Millman et al. (24), we estimate the solution osmotic pressure of a 10% dextran T-500 solution to be ~160 Torr. Applying this to Millman and Irving's (1988) Fig. 2 (25) for relaxed frog sartorius muscle in the same solution, we estimate that the myofilament lattice spacing decreases from 47.5 to 37.3 nm. Though the absolute lattice is different from rat cardiac muscle (16), the 21.5% decrease is very close to our findings (21.0%). But the slopes are slightly different (-0.1 in cardiac vs. -0.125 in skeletal). Because the same solutions are used, this difference is a real difference in muscle types and is not due to any apparent osmotic pressure difference. In other skeletal muscle studies, Umazume et al. (35) report a smaller initial lattice spacing (41.3 nm) and a greater compression (28%) in 10% PVP in their single frog semitendinosus fibers even after a precompression. The issue is even less clear with skeletal single fiber width data where 10% polymer concentrations elicit 29–39% compressions (9, 12, 13, 20, 34). These data suggest the possibility that the cardiac myofilament lattice is less compressible than skeletal muscles at a given solution osmotic pressure in the same polymer and that the large interfield spaces in heart muscle do not compress proportionally.

Longitudinal stability

There were no significant changes in unrestrained myocyte sarcomere lengths or in their distribution (Fig. 4). Skinned cells were only compressed radially with no visible alteration to longitudinal organization in any location within the cell. This is different than what is seen in intact cells where hypertonic saline solutions compressed the cell both radially and longitudinally (29). It is also different from the shortening behavior seen in skinned relaxed cells during myofilament extraction (32). Clearly, the stresses of radial compression elicited by PVP and dextran upon the myofilament lattice are not transferred to any longitudinal cytoskeletal component at L_0 as may be the case in intact cells and with myofilament extraction. This may not be the case at extended lengths where Higuchi (10) has shown there is a resting tension dependence upon lattice spacing in skeletal muscle.

Stiffness changes

Stiffness increases substantially when the myofilament lattice is compressed (Figs. 5 and 6). The majority of this increase occurs at higher concentrations of polymer (solution osmotic pressures) where the myofilament lattice is compressed to values significantly less than seen in the intact cell. The plots of stiffness as a function of cell width (Fig. 6) particularly emphasize this point. In modelling the skeletal muscle lattice spacing with osmotic compression, Millman and Irving (25) find a large increase in the slope of the lattice spacing-osmotic pressure relation at ~20 Torr. When the muscle diameter is initially decreased in a rigor state, little further change in diameter occurs until the pressure is increased above 20–100 Torr. At higher pressures, the slopes of the curves in relaxed and rigor skeletal muscles are similar. They interpret these findings to suggest that in the lower range of osmotic pressure (0–20 Torr) in relaxed muscle, the cross-bridges become increasingly compressed against the backbone of the thick filaments primarily by electrostatic repulsive forces between the contractile filaments. Over this range of pressures, there is a considerable decrease in diameter, but contractile filament interaction is minimal. Hence, longitudinal stiffness would not rise appreciably. With further compression at presures above 20–100 Torr, contractile filament interaction (viscoelastic, rather than attachment) increased dramatically. This interpretation would fit our results in cardiac cells (Fig. 6) because a large increase in slope of the stiffness-width relation occurs at about the 4% concentrations or 20 Torr.

The two phase stiffness-width relationship (Fig. 6) is also similar to most other skeletal muscle studies (12, 34, 35). Umazume et al. (35), using Brij-58 skinned semitendinosus fibers, and Tsuchiya (34) using mechanically skinned semitendinosus or aductor magnus muscles, showed that stiffness did not increase until the concentration of dextran reached ~4%. But their relative skeletal muscle cell diameter was compressed to ~0.78 of control as opposed to our 0.86 in cardiac myocytes at this polymer concentration. This two phase width-stiffness relationship is in contrast to data reported by Berman and Maughan (1) who showed a nearly linear relation between the elastic modulus and cell width in detergent-skinned frog semitendinosus in dextran T-500 solutions. The main procedural difference in the preparations is that Berman and Maughan prepared their fibers in mineral oil.

The stiffness-concentration data of Figure 5 is replotted in Fig. 7 with the initial resting stiffness at each cell length

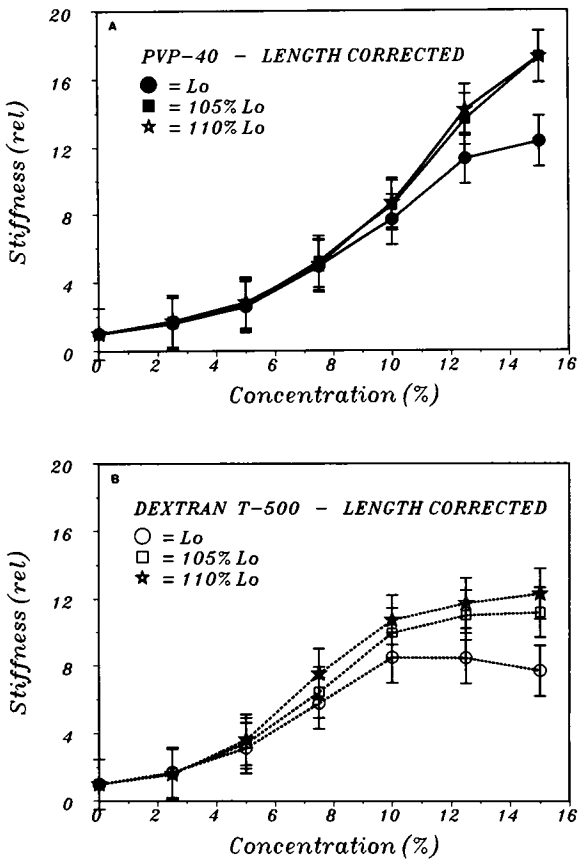

FIGURE 7 Length corrected stiffness relationship. The polymer concentration-stiffness relationships from Fig. 5 are replotted for PVP (*A*) and dextran (*B*) after length correction. The incremental passive stiffness increase at each length in 0% control solution is subtracted from each subsequent stiffness value at the same length in higher polymer concentrations.

subtracted from subsequent stiffness responses. Above the control length, the relations in both PVP and dextran solutions superimpose within experimental error. At the control length in the higher osmotic pressure media, the deviation is substantial, but may again reflect the tendency for the cell to sag at the higher osmotic pressures. With 5% stretch (105% L_0) the tendency to sag becomes less significant. Thus, the difference in stiffness with further length increase appears to be due entirely to the increase in passive stiffness rather than a differential effect related to osmotic pressure once the cell is stretched sufficiently taut to avoid the sag at control length.

The leveling off of the stiffness in high concentrations (>10%) of dextran is probably due to some elongation of the attached and perturbated cell at unstretched lengths. If the radial compression of dextran forces the cell to a longer length, then the apparent passive stiffness would be lower at any given length and sagging might appear upon return to the original L_0. A similar stiffness drop also appears to occur in relaxed glycerinated rabbit psoas fibers (Fig. 4 *B* of Kawai and Schulman, 1985, reference 12) bathed in 16% dextran. Interestingly, this effect is not seen in PVP compressions even though the solution osmotic pressures at any given concentration are higher in PVP than in dextran (24, 36). These data suggest that PVP is not perfectly excluded or not excluded as well as dextran from the myofilament lattice. If this is the case, estimated solution osmotic pressures may not indicate the real osmotic pressure within the muscle system. Thus, dextran may in fact exert the same or a greater osmotic pressure within the cell. This may be a contributing factor in the attached cell sagging in high dextran concentrations.

Ultrastructural considerations

These analyses suggest that skinned relaxed cardiac myocytes respond qualitatively, but not necessarily quantitatively, the same to osmotic compression with long-chain polymers as skeletal muscle fibers. A similar response to osmotic compression is not necessarily expected because of the vast differences between the field structure organization of cardiac muscle and fiber structure organization in skeletal muscle (3, 22, 26). There are probably few differences in the myofilament lattice structure itself as indicated by the qualitative similarity in cardiac and skeletal muscle x-ray diffraction patterns (16, 17). But there are specific differences in absolute lattice spacing (15–18, 24, 25, 28, 35) and probable cross-bridge movement (16) between resting skinned skeletal and cardiac preparations. Many of these differences are likely due to differences in the animal model, muscle lengths, or other experimental conditions. But there are several notable

differences in cellular organization between cardiac and skeletal muscle that can explain some of our observations.

The composition and distribution of cardiac cytoskeletal components is different from skeletal muscle (27). This is manifest in cardiac muscle's characteristic "field structure" of myofilamentous masses interspersed with large quantities (34–38%) of mitochondria vs. skeletal muscle's "fiber structure" of closely coupled myofibrils (3, 22, 26). Unlike in skeletal muscle, the 8% myofilament lattice swelling seen in the cardiac muscle by Matsubara et al. (16) cannot be adequately monitored by cell width measurements. We found precompression of the cardiac cell essential to establish stable control values. The precompression effect may be more dramatic in the cardiac cells because the myofilaments make up 80–87% of the cell volume in skeletal muscle (3), whereas they are only 48–54% of the volume in cardiac cells (3, 22, 26).

This same argument applies to the two phase width-stiffness discussion (above) where the measured cell widths compressed more in skeletal (34, 35) than in our cardiac data in 4% dextran. The ratio of the change in diameter is ~1.57 (0.22/0.14). This difference in diameter change can be approximately accounted for from the difference in myofilament content of the two types of muscle (3, 22, 26). Taking a midrange value for each proportion (84% skeletal to 51% cardiac), the ratio of myofilaments in skeletal to cardiac muscle is ~1.65. In 10% solution, the diameter changes were ~35% in skeletal muscle compared with the 21% in our study. This ratio is 1.67 indicating again that the lattice spacing changes are likely the same in the two types of muscle. On the other hand, the rather precise agreement in 10% solution may be somewhat fortuitous because the change in cardiac cell diameter may include an additional component of organelle loss by squeezing in the higher osmotic media.

Our observed differences in myofilament compressibility and stiffness could also be due to x-ray diffraction insensitive differences in charge distribution along or in the cytoskeletal structures associated with the interdigitating myofilaments. Irving and Millman (11) have rigorously modeled the thick/thin filament positions, diameters, and electron densities from their x-ray diffraction data of skeletal muscle. They have not directly addressed the possible contribution of the megadalton proteins of titin (connectin) and nebulin which are associated with the thick and thin filaments (14, 37). What role these cytoskeletal filaments play in myofilament charge distribution and therefore osmotic compression is not known. But Wang and Wright (37) have shown that titin is present in both cardiac and skeletal muscle whereas nebulin is found only in skeletal muscle I-bands. Furthermore, titin is believed to be one of the major contributors to passive resting tension in muscle (2, 14, 21, 37). Because the resting tension in cardiac muscle is substantially greater than in skeletal and the titin molecule appears to be similar in both muscle types, there may be some structural or attachment difference within the myofilament lattice. Other cytoskeletal components which are not directly associated with the myofilament lattice (e.g., intermediate filaments of the Z-disk) are less likely to contribute to these observed differences near L_0 because there appears to be little or no relationship between compression and longitudinal stability in these cells (except at high dextran concentrations).

We wish to thank Dr. Ichiro Matsubara of the University of Tohoku School of Medicine, Japan and Dr. David W. Maughan of the University of Vermont, USA for sharing their myofilament lattice compression data from rat cardiac muscle with us and for kindly reviewing this manuscript. The technical assistance of Peter Billings, Bob James, David Lake, Bradford Lubell, Audrey Matsumoto, Hans Poggemeyer, Norman Thot, and Elizabeth Wilks was invaluable in the preparation of the heart cells, solutions, data and photo processing, and software development. We thank Leota Green for final manuscript preparation.

This work was supported by National Heart, Lung, and Blood Institute grant HL-29671, grant 695-G1-3 from the American Heart Association, Greater Los Angeles Affiliate, and the Laubisch Endowment to Dr. Roos, and National Heart, Lung, and Blood Institute grant HL-30828 to Dr. Brady.

Received for publication 27 March 1990 and in final form 14 July 1990.

REFERENCES

1. Berman, M. R., and D. W. Maughan. 1982. Axial elastic modulus as a function of relative fiber width in relaxed skinned skeletal muscle fibers. *Pfluegers Arch. Eur. J. Physiol.* 393:99–103.
2. Brady, A. J., and S. P. Farnsworth. 1986. Cardiac myocyte stiffness following extraction with detergent and high salt concentrations. *Am. J. Physiol.* 250(Heart Circ. Physiol. 19): H932–H943.
3. Eisenberg, B. R. 1983. Quantitative ultrastructure of mammalian skeletal muscle. *In* Handbook of Physiology, Section 10: Skeletal Muscle. L. D. Peachey, R. H. Adrian, and S. R. Geiger, editors. American Physiological Society, Bethesda, MD. 73–112.
4. Fabiato, A., and F. Fabiato. 1978. Myofilament-generated tension oscillations during partial calcium activation and activation dependence of the sarcomere length-tension relation of skinned cardiac cells. *J. Gen. Physiol.* 72:667–699.
5. Fabiato, A., and F. Fabiato. 1979. Calculator programs for computing the composition of the solutions containing multiple metals and ligands used for experiments in skinned muscle cells. *J. Physiol. (Paris).* 75:463–505.
6. Fish, D., J. Orenstein, and S. Bloom. 1984. Passive stiffness of isolated cardiac and skeletal myocytes in the hamster. *Circ. Res.* 51:117–130.
7. Godt, R. E., and D. W. Maughan. 1977. Swelling of skinned fibers of the frog. Experimental observations. *Biophys. J.* 19:103–116.
8. Godt, R. E., and D. W. Maughan. 1981. Influence of osmotic compression on calcium activation and tension in skinned muscle fibers of the rabbit. *Pfluegers Arch. Eur. J. Physiol.* 391:334–337.

9. Gulati, J., and A. Babu. 1985. Critical dependence of calcium-activated force on width in highly compressed skinned fibers of the frog. *Biophys. J.* 48:781–787.

10. Higuchi, H. 1987. Lattice swelling with the selective digestion of elastic components in single-skinned fibers of frog muscle. *Biophys. J.* 52:29–32.

11. Irving, T. C., and B. M. Millman. 1989. Changes in thick filament structure during compression of the filament lattice in relaxed frog sartorius muscle. *J. Muscle Res. Cell Motil.* 10:385–394.

12. Kawai, M., and M. T. Schulman. 1985. Crossbridge kinetics in chemically skinned rabbit psoas fibres when the actin-myosin lattice spacing is altered by dextran T-500. *J. Muscle Res. Cell Motil.* 6:313–332.

13. Krasner, B., and D. Maughan. 1984. The relationship between ATP hydrolysis and active force in compressed and swollen skinned muscle fibers of the rabbit. *Pfluegers Arch. Eur. J. Physiol.* 400:160–165.

14. Maruyama, K., A. Matsuno, H. Higuchi, S. Shimaoka, S. Kimura, and T. Shimizu. 1989. Behavior of connectin (titin) and nebulin in skinned muscle fibres released after extreme stretch as revealed by immunoelectron microscopy. *J. Muscle Res. Cell Motil.* 10:350–359.

15. Matsubara, I., and G. F. Elliot. 1972. X-Ray diffraction studies on skinned single fibres of frog skeletal muscle. *J. Mol. Biol.* 72:657–669.

16. Matsubara, I., D. W. Maughan, Y. Saeke, and N. Yagi. 1989. Cross-bridge movement in rat cardiac muscle as a function of calcium concentration. *J. Physiol.* 417:555–565.

17. Matsubara, I., and B. M. Millman. 1974. X-Ray diffraction patterns from mammalian heart muscle. *J. Mol. Biol.* 82:527–536.

18. Matsubara, I., Y. Umazume, and N. Yagi. 1985. Lateral filamentary spacing in chemically skinned murine muscles during contraction. *J. Physiol.* 360:135–148.

19. Maughan, D., and M. Berman. 1982. Radial compression of functionally skinned cardiac bundles abolishes calcium activated force. *Biophys. J.* 37:363*a* (Abstr.)

20. Maughan, D. W., and R. E. Godt. 1979. Stretch and radial compression studies on relaxed skinned muscle fibers of the frog. *Biophys. J.* 28:391–402.

21. Maughan, D. W., and R. E. Godt. 1981. Radial forces within muscle fibers in rigor. *J. Gen. Physiol.* 77:49–64.

22. McNutt, N. S., and D. W. Fawcett. 1974. Myocardial ultrastructure. *In* The Mammalian Myocardium. G. A. Langer and A. J. Brady, editors. John Wiley & Sons, New York. 1–49.

23. Metzger, J. M., and R. L. Moss. 1987. Shortening velocity in skinned single muscle fibers. Influence of filament lattice spacing. *Biophys. J.* 52:127–131.

24. Millman, B. M., K. Wakabayashi, and T. J. Racey. 1983. Lateral forces in the filament lattice of vertebrate striated muscle in the rigor state. *Biophys. J.* 41:259–267.

25. Millman, B. M., and T. C. Irving. 1988. Filament lattice of frog striated muscle. Radial forces, lattice stability, and filament compression in the A-band of relaxed and rigor muscle. *Biophys. J.* 54:437–447.

26. Page, E., L. P. McCallister, and B. Power. 1971. Stereological measurements of cardiac ultrastructure implicated in excitation-contraction coupling. *Proc. Natl. Acad. Sci. USA.* 68:1465–1466.

27. Price, M. G. 1984. Molecular analysis of intermediate filament cytoskeleton—a putative load-bearing structure. *Am. J. Physiol.* 246 (Heart Circ. Physiol. 15):H566–H572.

28. Rome, E. 1972. Relaxation of glycerinated muscle: low-angle x-ray diffraction studies. *J. Mol. Biol.* 65:331–345.

29. Roos, K. P. 1986. Length, width, and volume changes in osmotically stressed myocytes. *Am. J. Physiol.* 251(Heart Circ. Physiol. 20):H1373–H1378.

30. Roos, K. P. 1986. Three-dimensional reconstructions of optically imaged single heart cell striation patterns. *Biophys. J.* 49:44–46.

31. Roos, K. P. 1987. Sarcomere length uniformity determined from three-dimensional reconstructions of resting isolated heart cell striation patterns. *Biophys. J.* 52:317–327.

32. Roos, K. P., and A. J. Brady. 1989. Stiffness and shortening changes in myofilament-extracted rat cardiac myocytes. *Am. J. Physiol.* 256(Heart Circ. Physiol. 25):H539–H551.

33. Roos, K. P., A. C. Bliton, B. A. Lubell, J. M. Parker, M. J. Patton, and S. R. Taylor. 1989. High speed striation pattern recognition in contracting cardiac myocytes. *Proc. Soc. Photo-Optical Instr. Eng.* 1063:29–41.

34. Tsuchiya, T. 1988. Passive interaction between sliding filaments in the osmotically compressed skinned muscle fibers of the frog. *Biophys. J.* 53:415–423.

35. Umazume, Y., S. Onodera, and H. Higuchi. 1986. Width and lattice spacing in radially compressed frog skinned muscle fibres at various pH values, magnesium ion concentrations and ionic strengths. *J. Muscle Res. Cell. Motil.* 7:251–258.

36. Vink, H. 1971. Precision measurements of osmotic pressure in concentrated polymer solutions. *Eur. Polym. J.* 7:1411–1419.

37. Wang, K., and J. Wright. 1988. Architecture of sarcomere matrix of skeletal muscle: immunoelectron microscopic evidence that suggests a set of parallel inextensible nebulin filaments anchored at the Z line. *J. Cell. Biol.* 107:2199–2212.